# Monitoring of ice growth on the East channel and on shallow lakes in the Mackenzie Delta

Anna Wendleder, German Aerospace Center (DLR), Anna.Wendleder@dlr.de, Germany
Achim Roth, German Aerospace Center (DLR), Achim.Roth@dlr.de, Germany
Andreas Schmitt, German Aerospace Center (DLR), Andreas.Schmitt@dlr.de, Germany

## Abstract

The global warming has a substantial impact on the local geomorphological system of the arctic environment. Earth observation data has the capacity to provide accurate high resolution information. Due to the all-weather and day and night observation capability Synthetic Aperture Radars (SAR) are particularly well suited for the mapping and monitoring of arctic and isolated environments. This paper presents the idea of a SAR-post processing system and the corresponding results that were achieved using a time series of dual-pol TerraSAR-X data from Mackenzie Delta. It comprises Kennaugh decomposition, ortho-rectification, radiometric enhancement, normalization and the classification of different ice types.

## 1 Introduction

During the melt season in 2012 the ice extent in the Arctic Ocean lost a total of 11.83 million square kilometres. This is the largest seasonal loss of sea ice in the satellite records [1]. This phenomenon is affected by the global warming. At Tuktoyaktuk, Beaufort Sea, Canada, an increase of the mean annual temperature of approx. 3° C between 1956 and 1993 has been measured [2]. These changes have a substantial impact on the local geomorphological system: the mean annual extent and duration of coverage of snow and sea ice reduces and hence the albedo effect decreases, the region sea level rises and the rates of erosion and the effects of storm surges increase. Particular, the southern Beaufort Sea is susceptible to these effects, as shorelines are typically ice-bonded and unconsolidated, making them more susceptible to thermal and mechanical erosion [3] [4].
Remote Sensing has the capacity to provide accurate high resolution information of the sea and land surface in an automated and standardized way. In particular satellites equipped with Synthetic Aperture Radars (SAR) enable regular mapping and monitoring of temporal variations in land cover and ice types. Their all-weather and day and night observation capability is an important advantage in the Arctic due to low illumination during winter period. In 2007 the German Earth Observation satellite TerraSAR-X was launched that provides high resolution dual-polarized SAR data. Since 2010 it is flying together with its twin satellite TanDEM-X in close formation enabling single pass interferometry. The primary mission goal is the generation of a global digital elevation model (DEM) in outstanding quality and resolution that allows classifying the shoreline and land's topography at an unprecedented level of detail.

Objective of this work is to develop higher level products of Polarimetric SAR (PolSAR) and DEM data that abet the characterization and accurate classification of arctic surface features for large areas. The higher level products are developed and proved in collaborative application projects. The proposed presentation shall provide information and ideas about the intended higher level products, their generation and provision will be supplemented by exemplary products.

## 2 Test Site

The test site is the East Channel of the Mackenzie Delta. The Mackenzie Delta is situated in the Beaufort Sea region of the Arctic Ocean at approximately 69° N and 133° W. For approximately eight months of the year the mean air temperatures remain below 0° C and for an average of six months per year the annual sea ice remains above 90% cover [5].

## 3 SAR Data

Six dual-pol TerraSAR-X strip-map images are selected between September 26$^{th}$ and November 20$^{th}$ 2012. This time span covers the freezing of the East Channel. The TerraSAR-X data can be acquired with a pixel spacing of 2.5 m. For this application a pixel spacing of 12 m is sufficient and consequently the radiometric stability is increased. All images are acquired co-polarized with the HH and VV channels. In order to have the same acquisition geometry, the same orbit with an incidence angle of 34° is used.
In the "DEM Mosaicking and Calibration Processor" the interferometric DEMs are mosaicked and calibrated to the TanDEM-X DEM with a pixel spacing of

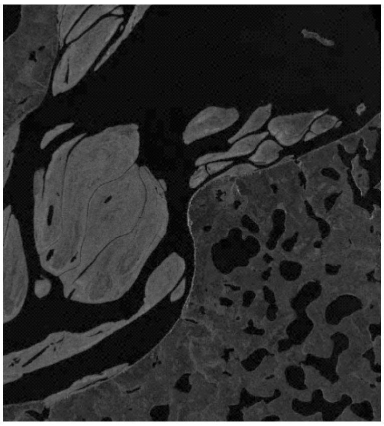

**Figure 1:** $K_0$ image of 2012/10/07.

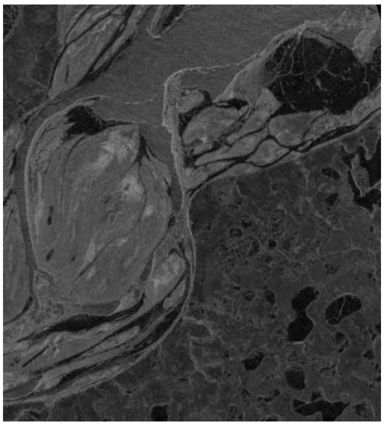

**Figure 2:** $K_0$ image of 2012/10/29.

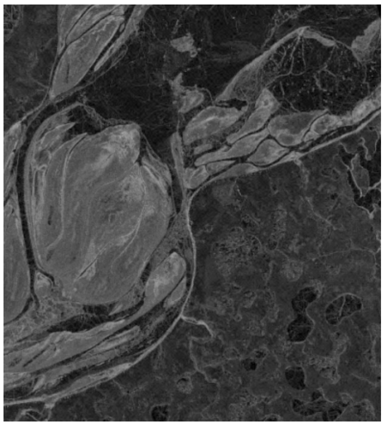

**Figure 3:** $K_0$ image of 2012/11/09.

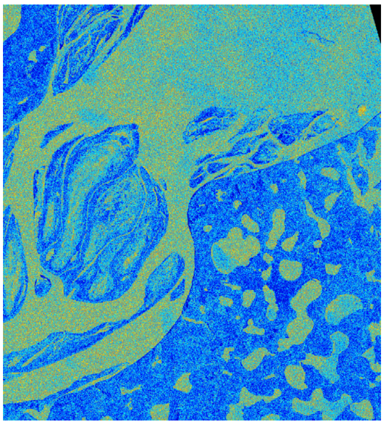

**Figure 4:** $K_3$ image of 2012/10/07.

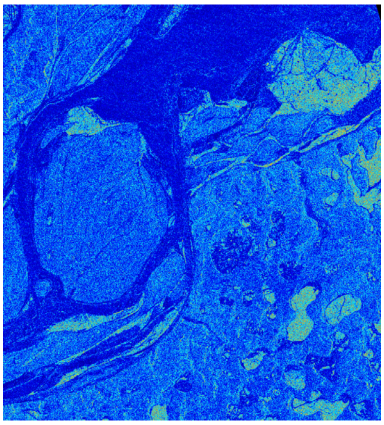

**Figure 5:** $K_3$ image of 2012/10/29.

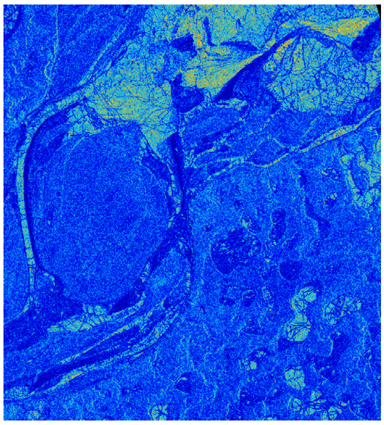

**Figure 6:** $K_3$ image of 2012/11/09.

12 m [6]. The data are acquired between January 29th and March 14th 2011. Usually, water surfaces show lower coherence in an interferometric data set due to temporal de-correlation and low backscattering. Consequently, the corresponding elevation values derived from the interferogram are random and produce a virtual relief. Since the water in the Mackenzie Delta is frozen during the acquisition time, the water surfaces are already flat and smooth, which means that an additional editing of the DEM is not required [7].

# 4 Methodology

The processing of the dual-pol TerraSAR-X data is divided into five main steps: Kennaugh decomposition, ortho-rectification, radiometric enhancement, normalization, the classification of different ice types and the separability analysis. In the last few years a lot of Polarimetric decompositions are developed. Due to the best representation of Polarimetric information the Kennaugh decomposition is chosen for this application. The ortho-rectification projects the Kennaugh elements from slant range to the earth's surface. The radiometric enhancement reduces the noise with the help of a multi-scale multi-looking process. The last steps are the classification of the different ice types and the separability analysis.

## 4.1 Kennaugh Decomposition

The Kennaugh matrix describes the Polarimetric information comparable to the covariance and the coherence matrix. In contrast to other matrix representations, every Kennaugh element is a real number. Its elements are all intensity differences, only the first element represents the total intensity [8]. In the dual-co-pol case the Kennaugh elements reduces to four independent elements, whereas only two elements are meaningful for this purpose. The element $K_0$ contains the total intensity and $K_3$ contains the difference between odd and double bounce.

$$K_0 \approx I_{HH} + I_{VV} \qquad (1)$$

$$K_3 \approx I_{even} - I_{odd} \qquad (2)$$

where $I_{HH}$ and $I_{VV}$ are the HH and VV intensities and $I_{even}$ and $I_{odd}$ are the proportions of total observed backscatter, that can be attributed to even and odd bounce scattering.

### 4.2 Ortho-rectification

Due to the side looking geometry of SAR-systems undulated terrain is significantly distorted during the SAR mapping process. The most important and well-known local images distortions are foreshortening, layover and shadow [9]. But also the range displacement effect needs to be considered that causes elevated features to be mapped in false range position. These effects as well as the varying ground resolution caused by varying slopes can be corrected during the ortho-rectification using a digital elevation model. In this case the TanDEM-X DEM is used. The technique of the ortho-rectification is explained in detail in [10] [11].

### 4.3 Radiometric-Enhancement

SAR images are inherently affected by a multiplicative deterministic noise called speckle and an additive stochastic noise referred to as thermal noise. All four polarizations are influenced by the noise separately [12]. Though the multi-scale multi-looking approach developed by Schmitt [13] applied individual to each image product improves the radiometric enhancement.

### 4.4 Normalization

The next step is the normalization of the output images. With the help of the hyperbolic tangent function, the floating point backscattering values, given in dB, are scaled to a value range from -1 to 1. This method enables no loss of information. The advantage is the comparison of images to different times independent of sensor or polarization.

### 4.5 Classification of ice types

Based on the intensity in $K_0$ and the backscattering values in $K_3$ elements three different ice types are classified. Therefor the maximum likelihood method is applied. The three different classes are smooth, consolidated and rough ice. Smooth ice features a low intensity and a low double bounce scattering, while consolidated ice features a low to medium intensity and a strong surface scattering. Rough ice shows a strong intensity and a strong surface scattering.

### 4.6 Separability Analysis

The separability analysis evaluates the statistical separability of the classification results, i.e. the information content of every class, and assesses the potential of different classification parameters. In this case the features of Jeffries-Matusita are applied. The values vary non-linearly between 0 and 2, whereas 1.9 and 2.0 are considered excellent and values smaller than 1.5 indicate low accuracy.

## 5 Results

For all six dual-pol TerraSAR-X images the Kennaugh elements are calculated. For the monitoring of the freezing of the Mackenzie Delta the $K_0$ and the $K_3$ element provide important and meaningful information. Due to the high resolution of the dual-pol TerraSAR-X data a lot of details can be identified. Figures 1 - 3 show the exemplarily three images of the $K_0$ elements of the East Channel between October 7$^{th}$ and November 9$^{th}$ 2012, Figures 4 - 6 show the corresponding images of the $K_3$ elements. The blue color describes odd bounce; the red color describes double bounce. The acquisition of the October 7$^{th}$, the $K_0$ images (Figure 1) show perfect smooth water. The entire transmitted signal is reflected away from the sensor and only a low backscatter value is received from the instrument, which affects in a higher double bounce in the $K_3$ images (Figure 3). During the acquisitions of October 29$^{th}$ and November 9$^{th}$ (Figure 2 - 3 and Figure 5 - 6) the process of the freezing can be monitored as the backscatter of the water changes from odd bounce to double bounce. Primarily, the shallow and offshore water freeze up subsequently the deep water. Accordingly, the time stamp of the freezing can be used for the estimation of the water depth and for the detection of the current. Additionally, in Figure 6 the forming and the borders of the ice floe are clearly visible.

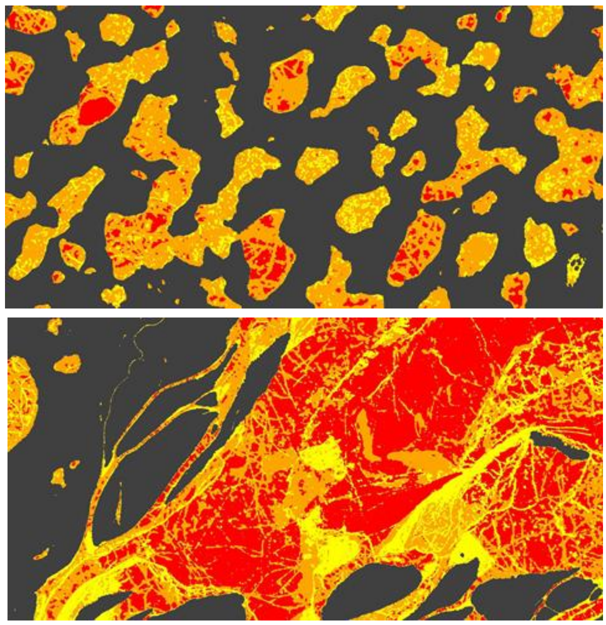

**Figure 7:** Ice Classification of 2012/11/09 (smooth ice displayed in red, consolidated ice in orange and rough ice in yellow).

Figure 7 shows the preliminary classification result between smooth (displayed in red), consolidated (displayed in orange) and rough ice (displayed in yellow) of the image on November 9$^{th}$. Along the seashore and the coast of the shallow lakes only rough and consolidated ice is detected, whereas inside of the East Channel and the shallow lakes only new and smooth ice is detected.

The separability analysis is calculated for every TerraSAR-X image. Table 1 shows representable the results of the separability analysis of the TSX image acquired on the 2012/11/09. The values range from 1.8 and 2.0 which means that the three different ice classes can be separated of each other with a high accuracy.

| | Ice 1 (smooth) | Ice 2 (consolidated) | Ice 3 (rough) |
|---|---|---|---|
| Ice 1 (smooth) | | 1,999929 | 2,000000 |
| Ice 2 (consolidated) | 1,999929 | | 1,836441 |
| Ice 3 (rough) | 2,000000 | 1,836441 | |

**Table 1:** Results of the separability analysis of the TSX data acquired on the 2012/11/09.

## 6 Conclusion

Our technique containing the Kennaugh decomposition, ortho-rectification, radiometric enhancement and normalization is universal applicable for multi-sensor, multi-polarization and multi-temporal processing provides important and meaningful information for the monitoring of arctic environments. The calibrated and ortho-rectified imagery, i.e. the intensity images and Kennaugh elements, are delivered. The compatibility of further decomposition processing like Freeman-Durden is ensured. The goal is to offer this post processor system to the users as add on to the standard level 1b processing presented.
The classifications of different ice types based on the Kennaugh elements show an application area for our technique with the primarily goal to understand better the freezing process of the East Channel and of the circumjacent shallow lakes. The object is to classify more ice types like frazil ice and ice with bubbles and to compare the freezing process between winter 2012 and winter 2013.

## References


[1] National Snow and Ice Data: *http://nsidc.org/arcticseaicenews/2012/10/poles-apart-a-record-breaking-summer-and-winter/* 2013 (last date accessed: 30.01.2013

[2] National Climate Data and Information Archieve: *http://climate.weatheroffice.gc.ca/climateData/canada_e.html* 2013 (last date accessed 30.01.2013)

[3] S. M. Solomon: *Spatial and temporal variability of shoreline change in the Beaufort-Mackenzie region, Northwest Territories*, Geo-Marine Letters 25 127-137, 2005

[4] J. R. Harper: *Morphology of the Canadian Beaufort Sea coast*, Marine Geology 91 75-91, 1990

[5] Canadian Ice Services (CIS): http://ice-glaces.ec.gc.ca/IceGraph103/page1.jsf, 2011 (last date accessed 11.07.2011)

[6] A. Gruber, B. Wessel, M. Huber, A. Roth: *Operational TanDEM-X DEM calibration and first validation results*, Journal of Photogrammetry and Remote Sensing 73 39-49, 2012

[7] A. Wendleder, B. Wessel, A. Roth, M. Breunig, K. Martin, S. Wagenbrenner: *TanDEM-X Water Indication Mask: Generation and First Evaluation Results*, Journal of Selected Topics in Applied Earth Observation and Remote Sensing 9 1-9, 2012

[8] S. R. Cloud: Polarisation- application in remote sensing, *Oxford University Press*, 2009

[9] G. Schreier: *Geometrical Properties of SAR Images*, SAR Geocoding and Systems 103-134, 1993

[10] A. Roth, M. Huber, D. Kosmann: *Geocoding of TerraSAR-X Data*, Proc. of 20'th International Congress of the ISPRS III 840-8444, 2004

[11] M. Huber, W. Hummelbrunner, J. Raggam, D. Small, D. Kosmann: *Technical Aspects of ENVISAT ASAR Geocoding Capability at DLR*, Proceedings of the 2004 ENVISAT & ERS Symposium, 2004

[12] A. Schmitt, A. Hogg, A. Roth: *Shoreline classification using dual-polarized TerraSAR-X images*, Proceedings of the 9$^{th}$ European Conference on Synthetic Aperture Radar (EUSAR 2012), 2012

[13] A. Schmitt: *Änderungserkennung in multitemporalen und multi-polarisierten Radaraufnahmen*, *PhD-Thesis*, http://digbib.ubka.uni-karlsruhe.de/volltexte/1000025955, 2012